



An electrochemical nano-sensor for determination of hydrazine using modified electrode by $\text{La}_2\text{O}_3\text{-Co}_3\text{O}_4$ nanohybrids and ionic liquid

Monireh Nazari¹, Hamideh Asadollahzadeh^{1,*} , Mehdi Shahidi¹, Nahid Rastakhiz¹, and Sayed Zia Mohammadi²

¹Department of Chemistry, Faculty of Science, Kerman Branch, Islamic Azad University, P. O. Box 7635131167, Kerman, Iran

²Department of Chemistry, Payame Noor University, Tehran, Iran

Received: 16 April 2021

Accepted: 6 September 2021

Published online:
23 September 2021

© The Author(s), under exclusive licence to Springer Science+Business Media, LLC, part of Springer Nature 2021

ABSTRACT

A non-enzymatic electrochemical sensor (modified carbon paste electrode (CPE) using $\text{La}_2\text{O}_3\text{-Co}_3\text{O}_4$ nanocomposite and ionic liquid) was made for sensitive quantification of hydrazine. The scanning electron microscopic (SEM), X-ray powder diffraction (XRD) as well as Fourier transform infrared spectroscopy (FT-IR) were employed for finding the nanocomposite characteristics. The electrochemical measurements revealed that combination of $\text{La}_2\text{O}_3\text{-Co}_3\text{O}_4$ nanocomposite and ionic liquid and carbon paste showed very good voltammetric responses toward hydrazine oxidation with the broad linear ranges between 0.1 and 120.0 μM and low detection limit (DL) of 0.01 μM , and 203.6 $\mu\text{A mM}^{-1} \text{cm}^{-2}$ sensitivity. Then, hydrazine in different water samples was determined by the standard addition procedure. We observed reasonable findings with relative standard deviation (RSD) of less than 3.4% and 96.0–103.0% recovery for 5 parallel measurements. Hence, $\text{La}_2\text{O}_3\text{-Co}_3\text{O}_4/\text{CPE}$ can be considered as one of the novel platforms for hydrazine to be electrochemically detected.

1 Introduction

Hydrazine (N_2H_4) has an extensive application in different areas like industrial factories, pharmaceuticals, rocket propellants, photography chemicals as well as corrosive inhibitors [1–4]. Despite these numerous applications, N_2H_4 has been reported to be poisonous, carcinogenic and cyanogenetic [5–8] by the United States Environmental Protection Agency

(EPA) [9]. This material may lead to serious injuries to the liver, lungs, nervous system, spinal cord, pneumonia, kidney damaging and temporary blindness and dizziness [10, 11]. Moreover, severe exposures to hydrazine can lead to mortality [9, 12].

Because this material has been considered to be carcinogenic and mutagenic, experts in the field have considerably examined its determination [13, 14]. Therefore, various methods have been proposed for

Address correspondence to E-mail: asadollahzadeh90@yahoo.com

determination of this material, such as spectrophotometry [15], amperometry [16], titration [17], chemiluminescence [18], fluorimetry [19] as well as electroanalytical procedures [20–22]. Researchers have also presented some procedures other than electroanalytical ones that suffer from complexity, taking a lot of time to be performed, and incapability of determining the real-time concentration of N_2H_4 [23]. In fact, electrochemical approaches have provided opportunities for N_2H_4 determination that are cost-effective, sensitive, fast, and portable [24]. However, oxidation of hydrazine electrochemically because of the sluggish kinetics at the surface of the bare electrode was occurred in a high oxidation over-potential [25].

Hence, numerous studies addressed the elimination of the above challenge by chemical modification of surface of electrode using a novel group of materials, including metals and metal oxides [26, 27]. Today, the ability of modified electrodes to reduce over-potential and enhancing the oxidation currents has been proven [4, 28–47].

In this context, efforts have been made towards the development of different types of chemically modified electrodes based on nanostructure materials: Pt nanoparticles (NPs) supported on a nano porous gold electrode, reduced graphene oxide-cobalt oxide nano cube@gold nanocomposite, $NiCo_2O_4$ nano rod, carbon dots- Cu_2O/CuO , Co_3O_4/N -doped carbon nanocomposites, ZrO_2 NPs, $NiCo_2S_4$ porous sphere, Pt-Cu@silicon, Co-CeO₂ nanoflake, multilayered reduced graphene oxide/gold-palladium nanohybrid, Ag@C core-shell and poly (alizarin yellow R), Material of Institute Lavoisier-53(Fe), cobalt NPs intercalated nitrogen-doped mesoporous carbon nanosheet networks [47], etc.

Sensors have wide applications in various fields: gas detecting [48], ammonia sensors [49], H_2O_2 or nitrite detection [50], filed of piezoresistive pressure sensors [51], nitrogen oxide detection [52], in the field of medical care [53, 54], glyphosate detection [55], etc.

More recently, Co_3O_4 and La_2O_3 NPs in the field of microwave absorption were also attracted wide attention [56, 57]. Therefore, with respect to these reports, the modified carbon paste electrode using $La_2O_3-Co_3O_4$ nanocomposite and ionic liquid, should have potential applications in the microwave absorption.

As far as we know, there was no report on the hydrazine oxidation with the modified $La_2O_3-Co_3O_4$

nanoparticles-ionic liquid CPE (LaCoILCPE). The aim of this research is preparing of the LaCoILCPE as the novel electrode and assesses of its function for N_2H_4 determination. Then, applicability of the LaCoILCPE for voltammetric determination of hydrazine in the real samples was assessed.

2 Experimental

2.1 Devices and chemicals

Devices utilized in this research are similar to the devices reported in the previous article [58].

Hydrazine hydrate ($N_2H_4 \cdot H_2O$, 80%), Na_2HPO_4 and NaH_2PO_4 bought from Sigma Aldrich Company. Moreover, we employed Na_2HPO_4 and NaH_2PO_4 for preparing phosphate buffer (PB) supporting electrolyte solution. In addition, all chemical compounds used in this work was analytical grade. Notably, deionized water was used for preparation of all solutions.

2.2 $La_2O_3-Co_3O_4$ nanocomposite synthesis

According to the research design, at first $La_2O_3-Co_3O_4$ nanocomposite was synthesized according to the previous report [58]. Briefly, we dissolved 0.46 mol of cobalt acetate in a beaker containing 80 mL of deionized water into a reaction bath, and 0.18 mol of thiourea was added to it with stirring and lastly 19.76 mL of ammonia was added to this solution, and five minutes shake. In the next step, the bath temperature enhanced up to 80 °C to form precipitate. This mixture put aside overnight, and then filtered. The filtrate was washed with ethanol and dried using an oven at 90 °C for 4 h. The obtained powder was Co_3O_4 NPs.

Then, 50 mL deionized water was given in a beaker and 0.2 mol of lanthanum nitrate, 0.1 g of Co_3O_4 NPs was added to it. In the following, NaOH solution (1.5 M) were poured dropwise to this solution until the pH of the solution reached to 10. Then, temperature of the solution was increased up to 80 °C and stirred for 1 h. The final product ($La_2O_3-Co_3O_4$ nanocomposite) was centrifuged at 3000 rpm for fifteen minutes, and washed with deionized water many times and ultimately vacuum-dried at a temperature of 60 °C overnight.

2.3 Preparation process of the electrode

In order to prepare the modified electrode, 0.9 g graphite powder with 0.1 g of $\text{La}_2\text{O}_3\text{-Co}_3\text{O}_4$ was mixed into a mortar. Then, 0.5 mL of paraffin and 0.2 mL ionic liquid was poured and again mixed for fifteen minutes. In the next step, the resultant paste entered into a glass tube (10 cm long and 3.4 mm i.d.) and packaged. In the following, a copper wire was inserted into the paste to make an electrical connection. After that, the excess paste pressed out of the glass tube and for obtaining the renewable surface a weighing paper was used to polish it. Furthermore, we applied a similar approach for preparing the $\text{La}_2\text{O}_3\text{-Co}_3\text{O}_4$ nanocomposite CPE (LaCoCPE) without ionic liquid, ionic liquid paste electrode (ILCPE) without the $\text{La}_2\text{O}_3\text{-Co}_3\text{O}_4$ nanocomposite, as well as the bare CPE without ionic liquid and the $\text{La}_2\text{O}_3\text{-Co}_3\text{O}_4$ nanocomposite for comparison.

2.4 Preparation process of the real samples

The water samples were collected from different places and used a $0.45\ \mu\text{m}$ filter to filter them. In the next step, 10 mL of each water sample was transported into a 50 mL volumetric flask and diluted to the mark with PBS (pH of 7.0). Then, a certain volume of $100.0\ \mu\text{M}$ hydrazine standard solution was poured into each sample before performing filtration for preparing the spiked samples.

3 Results and discussion

3.1 Structure and morphology of the $\text{La}_2\text{O}_3\text{-Co}_3\text{O}_4$ nanocomposite

The morphology of the $\text{La}_2\text{O}_3\text{-Co}_3\text{O}_4$ nanocomposite was examined via SEM image (Fig. 1) and revealed that the nano- Co_3O_4 has layered morphology consisting of nanosheets as reported by another researcher [56]. On the other hands, the nano- La_2O_3 displaying ball-like particles, with diameters of 20–1000 nm as reported by another researcher [59]. Therefore, as can be seen in Fig. 1, the La_2O_3 NPs was formed on the surface of the Co_3O_4 NPs.

Figure 2 represents FT-IR spectra of the $\text{La}_2\text{O}_3\text{-Co}_3\text{O}_4$ nanocomposite ($400\text{--}4000\ \text{cm}^{-1}$). This spectrum showed two strong vibrational band at ~ 520 and $449\ \text{cm}^{-1}$, which is attributed to metal-O

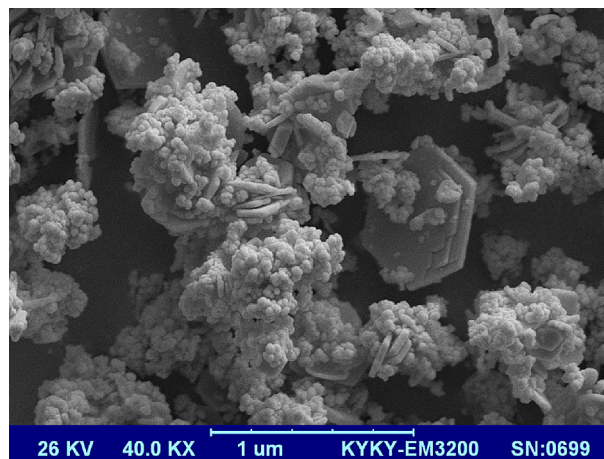


Fig. 1 The SEM image of $\text{La}_2\text{O}_3\text{-Co}_3\text{O}_4$ nanocomposite

vibration. Wide absorption peak appearing at nearly $3417\ \text{cm}^{-1}$ could be assigned to symmetric vibration of -OH groups of the absorbed H_2O molecules.

Figure 3 demonstrates outputs of XRD for the synthesized $\text{La}_2\text{O}_3\text{-Co}_3\text{O}_4$ nanocomposite. As shown in the figure, each major diffraction peak in the spectra represents a pure phase for $\text{La}_2\text{O}_3\text{-Co}_3\text{O}_4$ nanocomposite and is completely consistent with the sample standard peaks. The diffraction peaks at 31.7° , 36.1° , 44.5° , 59.9° and 64.9° corresponding to (220), (311), (400), (511) and (440) planes of Co for Co_3O_4 NPs (Fig. 3) corresponded to values from JCPDS 74–2120 [60].

Moreover, the diffraction peaks at 15.1° , 28.5° , 29.1° , 39.8° , 49.1° and 55.2° corresponding to (100), (002), (101), (102), (211) and (201) plane of La_2O_3 corresponded to values from JCPDS 41–4019.

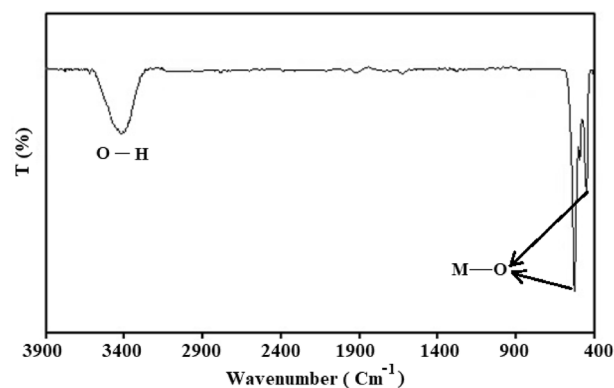


Fig. 2 The FT-IR image of $\text{La}_2\text{O}_3\text{-Co}_3\text{O}_4$ nanocomposite

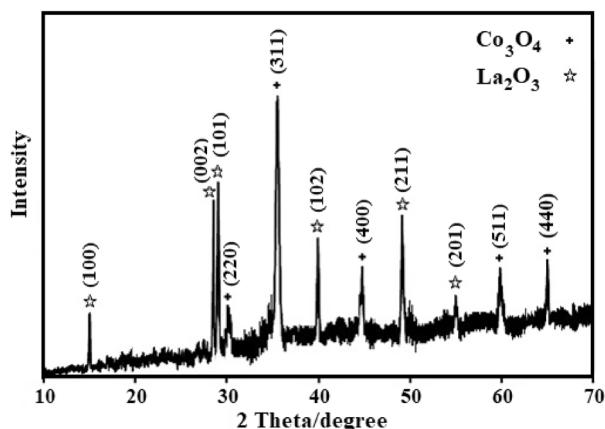


Fig. 3 The XRD pattern of the $\text{La}_2\text{O}_3\text{-Co}_3\text{O}_4$ nanocomposite

3.2 Electrochemical behavior of hydrazine at the LaCoILCPE surface

The obtained CVs for electrochemical oxidation of $50.0 \mu\text{M}$ hydrazine at the bare CPE, the LaCoCPE, the ILCPE, and the LaCoILCPE are presented in Figs. 4a, 4b, 4c and 4d, respectively.

As illustrated in the figure, the anodic oxidation potential of hydrazine at the surface of the LaCoILCPE and the bare CPE is 810 mV and 1060 mV , respectively, which reflects the capability of the $\text{La}_2\text{O}_3\text{-Co}_3\text{O}_4$ nanocomposite as well as IL as one of the proper mediators. Compared to the bare CPE, the anodic oxidation potential of hydrazine at the LaCoILCPE switched around 250 mV to negative values. Nonetheless, as compared to the bare CPE, the anodic peak current (curve *d*) considerably

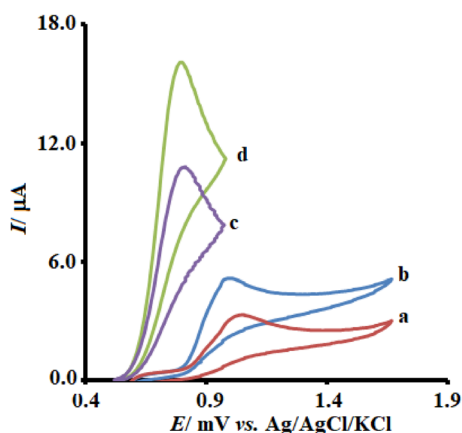


Fig. 4 The cyclic voltammograms of the unmodified CPE (*a*), the LaCoCPE (*b*), the ILCPE (*c*) and the LaCoILCPE (*d*) in the presence of $50.0 \mu\text{M}$ hydrazine into 0.1 M PBS (pH of 7.0). Scan rate equaled 50 mV/s in all cases

increased, which can be attributed to the probable electrocatalytic impacts of the LaCoILCPE on hydrazine.

In the next step, optimizing the solution pH would be crucial to achieve electrocatalytic oxidation of hydrazine. Therefore, the dependence of electrochemical activity of hydrazine on the pH value of the aqueous solution was also assessed. For this purpose, we used CV to investigate electrochemical activity of hydrazine into 0.1 M PBS with different pH-values ($3.0 < \text{pH} < 9.0$) at the LaCoILCPE surface. The results showed that the electrochemical oxidation of hydrazine at the LaCoILCPE surface in neutral conditions is better than acidic or alkaline conditions (Fig. 5). Therefore, pH of 7.0 was chosen as optimum pH for electrochemical oxidation of hydrazine at the LaCoILCPE surface.

3.3 Effects of the scan rate

The impact of the potential scan rates on the oxidation current of hydrazine was second parameter that was assessed (Fig. 6) and observed that with increase of the scan rate, the peak current was also enhanced. Due to the linear dependence of the anodic peak current (I_p) against the square root of the scanning rate ($v^{1/2}$), it can be concluded that oxidation process is diffusion-controlled.

In the following, using the data of the CV recorded at a scan rate of 10 mV s^{-1} , the TOEFL curve was plotted (Fig. 7). This section of voltammogram that is called Tafel region would be influenced by the electron transfer kinetic between substrate (hydrazine) and the LaCoILCPE. The Tafel slope is 0.1084 that completely match with the involvement of 1 electron in the rate-determining step of the electrode [61],

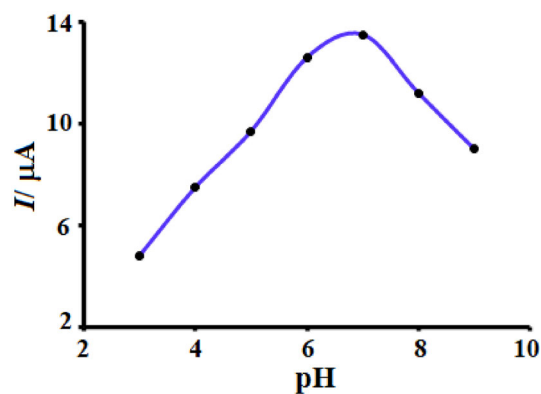


Fig. 5 The plot of I_p vs. pH

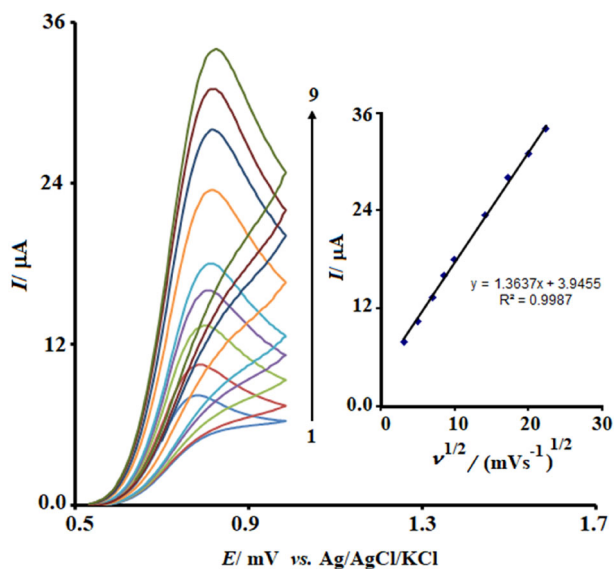


Fig. 6 CVs of the LaCoILCPE into 0.1 M PBS (pH of 7.0) containing 50.0 μM hydrazine at different scan rates. Notably, 1 to 9 are corresponding to 10, 25, 50, 75, 100, 200, 300, 400 and 500 mV s^{-1} . Inset: Variations in the anodic peak current versus the square root of the scan rates

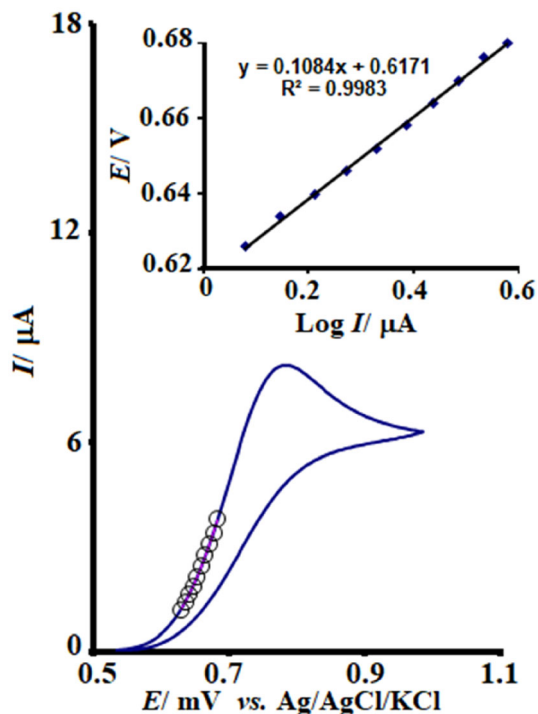


Fig. 7 A Tafel plot extracted from CV of the LaCoILCPE into 0.1 M PBS (pH of 7.0) containing 50.0 μM hydrazine at a scan rate equal to 10 mV s^{-1}

considering the charge transfer coefficient, $\alpha = 0.46$ for hydrazine.

3.4 Chronoamperometric measurement

In the next step, to perform the chronoamperometric measurements of hydrazine at the surface of the LaCoILCPE, the working electrode potential was adjusted at 900 mV versus Ag/AgCl/KCl (3.0 M) (Fig. 8). The current produced from electrochemical reaction at the mass transport limited condition for electroactive material (in this case: hydrazine), that having a diffusion coefficient of D can be ascribed by Cottrell equation [61]:

$$I = nFAD^{1/2}C_b\pi^{-1/2}t^{-1/2} \quad (1)$$

here C_b and D imply the bulk concentration (mM) and diffusion coefficient ($\text{cm}^2 \text{s}^{-1}$). The chronoamperometric measurements of hydrazine are performed in diverse concentrations of hydrazine (0.1 M of PBS at pH of 7.0). Then, the plots of I versus $t^{-1/2}$

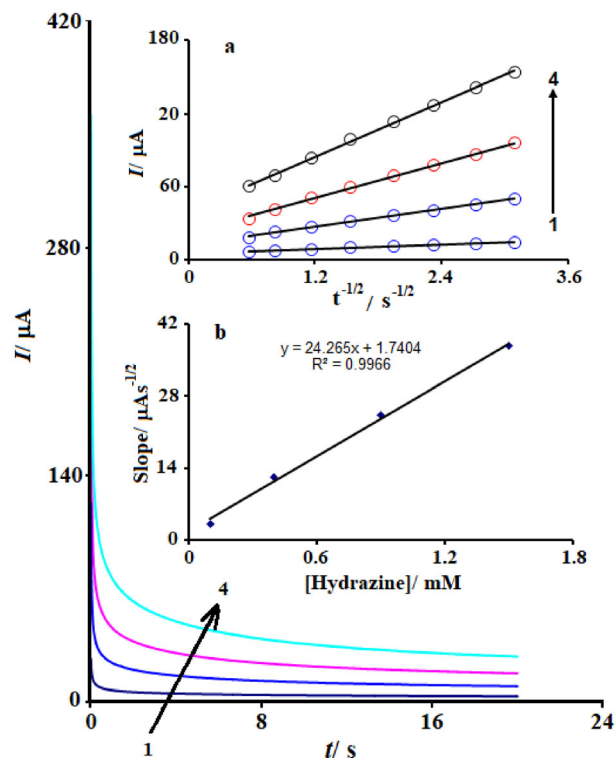


Fig. 8 Chronoamperograms observed at the LaCoILCPE into 0.1 M PBS (pH of 7.0) containing different concentrations of hydrazine. It is notable that 1 to 4 are corresponding to 0.1, 0.4, 0.9 and 1.5 mM of hydrazine. Inset: The plot of I versus $t^{-1/2}$ obtained from the chronoamperograms 1–4 (a), the slope of straight lines against concentration of hydrazine (b)

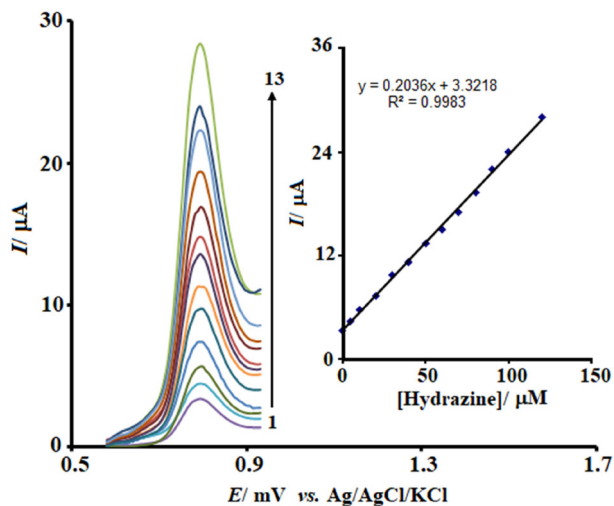


Fig. 9 The DPV of the LaCoILCPE into 0.1 M PBS (pH of 7.0) containing different concentrations of hydrazine (0.1, 5.0, 10.0, 20.0, 30.0, 40.0, 50.0, 60.0, 70.0, 80.0, 90.0, 100.0 and 120.0 μM). Inset: The peak current plot versus concentration of hydrazine in ranges from 0.1–120.0 μM

were plotted (Fig. 8a). In the following, the slopes of the resultant straight lines versus (Fig. 8b) concentration of hydrazine were plotted. Based on the final slope and the Cottrell equation, the mean value of D for hydrazine was calculated as $5.0 \times 10^{-5} \text{ cm}^2 \text{ s}^{-1}$

which is consistent with the reported results by another researchers [62, 63].

3.5 Calibration plot and detection limit

It is possible to use electrooxidation peak current of hydrazine at the LaCoILCPE surface for measurement of hydrazine in solution. Since DPV has a higher sensitivity compared to other quantitative methods, therefore, this method was used to investigate the linear range of the method. To perform this test, the LaCoILCPE was placed in a series of hydrazine solutions with different concentrations and peak current was measured. According to the findings (Fig. 9), the oxidation current of hydrazine at the LaCoILCPE surface has a linear dependence on the hydrazine concentration (at range 1.0×10^{-7} – $1.2 \times 10^{-4} \text{ M}$), with a correlation coefficient of 0.9983. Finally based on 3 s, a detection limit of $0.1 \times 10^{-7} \text{ M}$ for hydrazine was calculated.

Table 1 compares analytical function of the LaCoILCPE with the other modified electrodes [9, 30, 33, 36, 45, 47, 62, 64–68]. As seen in the table, the sensitivity, the detection limit and the linear range obtained using the LaCoILCPE is in the range of many reports or even better. As can be seen in

Table 1 The comparison of the effectiveness of some approaches employed to detect hydrazine

Method	Sensitivity ($\mu\text{A}/\mu\text{M cm}^2$)	LOD (nM)	Dynamic range (μM)	Refs
Reduced graphene oxide-cobalt oxide nanocube@gold nanocomposite/glassy carbon electrode	0.5830	443	10–620	[9]
Nanoporous gold electrode decorated with Pt nanoparticles	3.449	1030	5–6105	[30]
NiCo ₂ O ₄ nanorod/glassy carbon electrode	0.0482	260	10–2250	[33]
Carbon dots-Cu ₂ O/CuO/glassy carbon electrode	0.0044	24	0.99–5903	[36]
Au/Pd nanoparticles interleaved reduced graphene oxide/glassy carbon electrode	0.125	16	0.1–200	[45]
Material of Institute Lavoisier-53(Fe)/glassy carbon electrode	0.2122	30	0.25–380	[47]
Co ₃ O ₄ /N-doped carbon/ glassy carbon electrode	0.0566	110	0.5–977.4	[62]
Two new Cu(II) and Ni(II) complexes of a tetradentate N ₂ O ₂ Schiff base ligand/glassy carbon electrode	0.00487	166.66	0.5–150	[64]
Copper oxide anchored onto wormlike ordered mesoporous carbon/ glassy carbon electrode	0.1174	887	1–2110	[65]
Ag nanoparticles on nano cobalt-based metal organic framework//carbon paste electrode	0.0411	1450	4–326	[66]
Cu ₃ (BTC) ₂ /GO nanocomposite/glassy carbon electrode	–	500	1–5000	[67]
MoS ₂ /rGO)/Au/glassy carbon electrode	0.032	500	2–30	[68]
LaCoILCPE	0.2036	10.0	0.1–120	This work

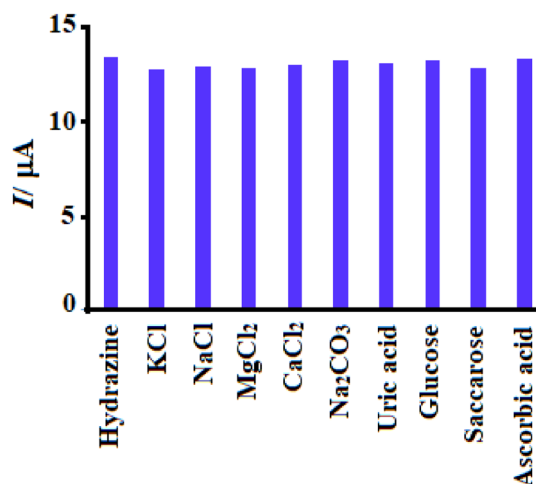


Fig. 10 The bar chart shows the current response of the LaCoILCPE to 50 μM of hydrazine coexisting in the solution with 0.5 mM of each interfering species (KCl, NaCl, MgCl₂, CaCl₂, Na₂CO₃, Uric acid, Glucose, Saccarose and Ascorbic acid)

Table 1, the LaCoILCPE sensor shows lower detection limit and higher sensitivity than others. The high sensitivity may be ascribed to the high porous structure of the La₂O₃-Co₃O₄ nanocomposite, which facilitates the transport of electroactive molecules. The low detection limit may be the result of the synergistic effect of the La₂O₃ NPs, the Co₃O₄ NPs and ionic liquid.

3.6 Reproducibility and stability

To evaluate the reproducibility of the LaCoILCPE sensor, DPV was used. The calculated RSD for ten measurements of 50 μM of hydrazine was 2.9%, which demonstrates reasonable reproducibility of the

LaCoILCPE sensor. For assessment of stability of the LaCoILCPE, a modified electrode was storage for 21 days, and then used for hydrazine determination. The obtained data showed that current response of the LaCoILCPE to the hydrazine after 21 days was 96.1% of its initial value, which illustrates a very good storage stability.

3.7 Interference effect

The interference effect is a very important factor in the analytical chemistry. For this research, we determined the impact of some possible interfering species on the detection of 50.0 μM hydrazine by DPV. Results (Fig. 10) were shown that tenfold KCl, NaCl, MgCl₂, CaCl₂, Na₂CO₃, Uric acid, Glucose, Saccarose and Ascorbic acid had no interference in detecting hydrazine, and the variation in the current caused by the interference species was less than ± 5%. Therefore, it can be concluded that, the LaCoILCPE enjoys an acceptable selectivity to detect hydrazine.

3.8 Real-sample analysis

For this step, the LaCoILCPE was employed to measure hydrazine in different water samples. After the sample pretreatment (Sect. 2.4), hydrazine was determined by DPV. Since, the real samples were assessed and are without hydrazine, therefore a known concentration of hydrazine was added into the samples and was determined by DPV. Table 2 gives the outputs and showed that the recoveries of this new method are in the range of 96.0–103.0%. Moreover, RSD values ($n = 5$) are < ± 3.4%,

Table 2 Utilization of the LaCoILCPE to detect hydrazine in the water samples ($n = 5$)

Sample	Spiked (μM)	Found (μM)	Recovery (%)	RSD (%)
River water	–	ND ^a	–	–
	10.0	9.8 ± 0.2	98.0	3.2
	20.0	19.3 ± 0.5	96.5	3.0
	50.0	51.4 ± 1.3	102.8	2.6
Well water	–	ND	–	–
	10.0	9.6 ± 0.2	96.0	2.9
	20.0	20.5 ± 0.4	102.5	2.6
	50.0	51.5 ± 1.4	103.0	3.1
Top water	–	ND	–	–
	10.0	9.9 ± 0.3	99.0	3.3
	20.0	19.6 ± 0.5	98.0	2.8
	50.0	50.5 ± 1.5	101.0	2.7

^aNot detect

demonstrating hydrazine detection in the water samples using the LaCoILCPE is highly reliable.

4 Conclusion

As mentioned earlier, we applied the $\text{La}_2\text{O}_3\text{-Co}_3\text{O}_4$ nanocomposite as well as an ionic liquid as the modifier for modification of carbon paste electrode, and designed a new sensor providing a sensitive approach to detect hydrazine. This new approach is simplified, portable, and economical to measure the concentration of hydrazine in different water samples with an acceptable analytical function. As a result of the good combination of $\text{La}_2\text{O}_3\text{-Co}_3\text{O}_4$ nanocomposite and ionic liquid, this sensor shows dramatic electrochemical activities for hydrazine oxidation.

Acknowledgements

The author is grateful to Islamic Azad University, Kerman Branch, for financial assistance of this work.

Declarations

Conflict of interest The authors declare that they have no competing interests.

References

1. R. Devasenathipathy, V. Mani, S.M. Chen, Highly selective amperometric sensor for the trace level detection of hydrazine at bismuth nanoparticles decorated graphene nanosheets modified electrode. *Talanta* **124**, 43–51 (2014)
2. J. Zhang, W.B. Gao, M.L. Dou, F. Wang, J.J. Liu, Z.L. Li, J. Ji, Nanorod-constructed porous Co_3O_4 nanowires: highly sensitive sensors for the detection of hydrazine. *Analyst* **140**, 1686–1692 (2015)
3. S. Zhao, L.L. Wang, T.T. Wang, Q.H. Han, S.K. Xu, A high-performance hydrazine electrochemical sensor based on gold nanoparticles/single-walled carbon nanohorns composite film. *Appl. Surf. Sci.* **369**, 36–42 (2016)
4. C. Duan, Y. Dong, Q. Sheng, J. Zheng, A high-performance non-enzymatic electrochemical hydrazine sensor based on NiCo_2S_4 porous sphere. *Talanta* **198**, 23–29 (2019)
5. M.B. Gholivand, A. Azadbakht, A novel hydrazine electrochemical sensor based on a zirconium hexacyanoferrate film-bimetallic Au-Pt inorganic-organic hybrid nanocomposite onto glassy carbon-modified electrode. *Electrochim. Acta* **56**, 10044–10054 (2011)
6. M. Mazloum-Ardakani, A. Khoshroo, An electrochemical study of benzofuran derivative in modified electrode-based CNT/ionic liquids for determining nanomolar concentrations of hydrazine. *Electrochim. Acta* **103**, 77–84 (2013)
7. Y. Wang, Y. Wan, D. Zhang, Reduced graphene sheets modified glassy carbon electrode for electrocatalytic oxidation of hydrazine in alkaline media. *Electrochem. Commun.* **12**, 187–190 (2010)
8. F. Luan, S. Zhang, D. Chen, K. Zheng, X. Zhuang, CoS_2 -decorated ionic liquid-functionalized graphene as a novel hydrazine electrochemical sensor. *Talanta* **182**, 529–535 (2018)
9. M.M. Shahid, P. Rameshkumar, W.J. Basirunc, U. Wijayantha, W.S. Chiu, P.S. Khiew, N.M. Huang, An electrochemical sensing platform of cobalt oxide@gold nanocubes interleaved reduced graphene oxide for the selective determination of Hydrazine. *Electrochim. Acta* **259**, 606–616 (2018)
10. L. Cui, C. Ji, Z. Peng, L. Zhong, C. Zhou, L. Yan, S. Qu, S. Zhang, C. Huang, X. Qian, Unique tri-output optical probe for specific and ultrasensitive detection of hydrazine. *Anal. Chem.* **86**, 4611–4617 (2014)
11. L. Cui, Z. Peng, C. Ji, J. Huang, D. Huang, J. Ma, S. Zhang, X. Qian, Y. Xu, Hydrazine detection in the gas state and aqueous solution based on the Gabriel mechanism and its imaging in living cells. *Chem. Commun.* **50**, 1485–1487 (2014)
12. G. Choudhary, H. Iansen, S. Donkin, C. Kirman, Toxicological profile for hydrazines. US Department of Health and Human Service, 5, (1997)
13. S. Dutta, C. Ray, S. Mallick, S. Sarkar, A. Roy, T. Pal, Au@Pd core-shell nanoparticles decorated reduced graphene oxide: a highly sensitive and selective platform for electrochemical detection of hydrazine. *RSC Adv.* **5**, 51690–51700 (2015)
14. H. Karimi-Maleh, M. Moazampour, A.A. Ensafi, S. Mallakpour, M. Hatami, An electrochemical nanocomposite modified carbon paste electrode as a sensor for simultaneous determination of hydrazine and phenol in water and wastewater samples. *Environ. Sci. Pollut. Res.* **21**, 5879–5888 (2014)
15. A.A. Ensafi, B. Rezaei, Flow injection determination of hydrazine with fluorimetric detection. *Talanta* **47**, 645–649 (1998)
16. D. Jayasri, S.S. Narayanan, Amperometric determination of hydrazine at manganese hexacyanoferrate modified graphite-wax composite electrode. *J. Hazard. Mater.* **144**, 348–354 (2007)

17. J.S. Budkuley, Determination of hydrazine and sulphite in the presence of one another. *Microchim. Acta* **108**, 103–105 (1992)
18. A. Safavi, M.A. Karimi, Flow injection chemiluminescence determination of hydrazine by oxidation with chlorinated isocyanurates. *Talanta* **58**, 785–792 (2002)
19. A. Safavi, A.A. Ensafi, Kinetic spectrophotometric determination of hydrazine. *Anal. Chim. Acta* **300**, 307–311 (1995)
20. Q. Yi, W. Yu, Nanoporous gold particles modified titanium electrode for hydrazine oxidation. *J. Electroanal. Chem.* **633**, 159–164 (2009)
21. D. Afzali, H. Karimi-Maleh, M.A. Khalilzadeh, Sensitive and selective determination of phenylhydrazine in the presence of hydrazine at a ferrocene-modified carbon nanotube paste electrode. *Environ. Chem. Lett.* **9**, 375–381 (2011)
22. A. Tahira, A. Nafady, M. Arain, S.T.H. Sherazi, T. Shaikh, Q. Baloach, M. Willander, Z.H. Ibupoto, The synthesis of new nanostructures of CuO using ascorbic acid as growth directing agent and their sensitive electrochemical detection of hydrazine. *Sens. Lett.* **14**, 611–615 (2016)
23. Y. Liu, Y. Li, X. He, In situ synthesis of ceria nanoparticles in the ordered mesoporous carbon as a novel electrochemical sensor for the determination of hydrazine. *Anal. Chim. Acta* **819**, 26–33 (2014)
24. C. Karupppiah, S. Palanisamy, S.-M. Chen, S.K. Ramaraj, P.A. Periakaruppan, novel and sensitive amperometric hydrazine sensor based on gold nanoparticles decorated graphite nanosheets modified screen-printed carbon electrode. *Electrochim. Acta* **139**, 157–164 (2014)
25. C. Zhang, G. Wang, Y. Ji, M. Liu, Y. Feng, Z. Zhang, B. Fang, Enhancement in analytical hydrazine based on gold nanoparticles deposited on ZnO-MWCNTs films. *Sens. Actuator B* **150**, 247–253 (2010)
26. P.K. Rastogi, V. Ganesan, S. Krishnamoorthi, Palladium nanoparticles decorated gaur gum-based hybrid material for electrocatalytic hydrazine determination. *Electrochim. Acta* **125**, 593–600 (2014)
27. J. Ding, S. Zhu, T. Zhu, W. Sun, Q. Li, G. Wei, Z. Su, Hydrothermal synthesis of zinc oxidereduced graphene oxide nanocomposites for an electrochemical hydrazine sensor. *RSC Adv.* **5**, 22935–22942 (2015)
28. S.Z. Mohammadi, H. Beitollahi, M. Askari, R. Hosseinzadeh, Application of a modified carbon paste electrode using core-shell magnetic nanoparticle and modifier for simultaneous determination of norepinephrine, acetaminophen and tryptophan. *Rus. J. Electrochem.* **57**, 74–84 (2021)
29. S. Tajik, H. Beitollahi, F. Garkani Nejad, K.O. Kirlikovali, Q. Van Le, H.W. Jang, R.S. Varma, O.K. Farha, M. Shokouhimehr, Recent electrochemical applications of metal-organic framework-based materials. *Cryst Growth Des.* **20**, 7034–7064 (2020)
30. Y. Pei, M. Hu, Y. Xia, W. Huang, Z. Li, S. Chen, Electrochemical preparation of Pt nanoparticles modified nanoporous gold electrode with highly rough surface for efficient determination of hydrazine. *Sens. Actuators B* **304**, 127416 (2020)
31. S.Z. Mohammadi, H. Beitollahi, M. Kaykhahi, N. Mohammadzadeh, S. Tajik, R. Hosseinzadeh, Simultaneous determination of doxidopa and carbidopa by carbon paste electrode functionalized with NiFe₂O₄ nanoparticle and 2-(4-ferrocenyl-[1,2,3] triazol-1-yl)-1-(naphthalen-2-yl) ethenone. *Measurement* **155**, 107522 (2020)
32. H. Beitollahi, F. Movahedifar, S. Tajik, S. Jahani, A review on the effects of introducing CNTs in the modification process of electrochemical sensors. *Electroanalysis* **31**, 1195–1203 (2019)
33. V. Sudha, S.M. SenthilKumar, R. Thangamuthu, NiCo₂O₄ nanorod: synthesis and electrochemical sensing of carcinogenic hydrazine. *Inorg. Chem. Commun.* **116**, 107927 (2020)
34. H. Mahmoudi-Moghaddam, S. Tajik, H. Beitollahi, A new electrochemical DNA biosensor based on modified carbon paste electrode using graphene quantum dots and ionic liquid for determination of topotecan. *Microchem. J.* **150**, 104085 (2019)
35. S.Z. Mohammadi, H. Beitollahi, N. Mohammad Rahimi, Voltammetric determination of epinephrine and uric acid using modified graphene oxide nano sheets paste electrode. *J. Anal. Chem.* **74**, 345–354 (2019)
36. G. Wei, L. Wang, L. Huo, Y. Zhang, Economical, green and rapid synthesis of CDs-Cu₂O/CuO nanotube from the biomass waste reed as sensitive sensing platform for the electrochemical detection of hydrazine. *Talanta* **209**, 120431 (2020)
37. H. Beitollahi, M.A. Khalilzadeh, S. Tajik, M. Safaei, K. Zhang, H. Won Jang, M. Shokouhimehr, Recent advances in applications of voltammetric sensors modified with ferrocene and its derivatives. *ACS Omega* **5**, 2049–2059 (2020)
38. S.Z. Mohammadi, H. Beitollahi, Z. Dehghan, R. Hosseinzadeh, Electrochemical determination of ascorbic acid, uric acid and folic acid using carbon paste electrode modified with novel synthesized ferrocene derivative and core-shell magnetic nanoparticles in aqueous media. *Appl. Organometal. Chem.* **32**, 4551 (2018)
39. A.A. Ensafi, M.M. Abarghoui, B. Rezaei, Facile synthesis of Pt-Cu@silicon nanostructure as a new electrocatalyst supported matrix, electrochemical detection of hydrazine and hydrogen peroxide. *Electrochim. Acta* **190**, 199–207 (2016)
40. S. Tajik, Z. Dourandish, K. Zhang, H. Beitollahi, Q. Van Le, H. Won Jang, M. Shokouhimehr, Carbon and graphene quantum dots: a review on syntheses, characterization,

- biological and sensing applications for neurotransmitter determination. *RSC Adv.* **10**, 15406–15429 (2020)
41. S.Z. Mohammadi, H. Beitollahi, M. Kaykhaii, N. Mohammadzadeh, A novel electrochemical sensor based on graphene oxide nanosheets and ionic liquid binder for differential pulse voltammetric determination of drosidopa in pharmaceutical and urine samples. *Rus. J. Electrochem.* **55**, 1229–1236 (2019)
 42. M.R. Ganjali, H. Salimi, S. Tajik, H. Beitollahi, M. Rezapour, B. Larijani, Application of $\text{Fe}_3\text{O}_4/\text{SiO}_2/\text{MWCNT}$ film on glassy carbon electrode for the sensitive electroanalysis of levodopa. *Int. J. Electrochem. Sci.* **12**, 5243–5253 (2017)
 43. S. Esfandiari Baghbamidi, H. Beitollahi, S. Tajik, R. Hosseinzadeh, Voltammetric sensor based on 1-Benzyl-4-ferrocenyl-1H- [1,2,3]-triazole /carbon nanotube modified glassy carbon electrode; detection of hydrochlorothiazide in the presence of propranolol. *Int. J. Electrochem. Sci.* **11**, 10874–10883 (2016)
 44. H. Beitollahi, H. Mahmoudi Moghaddam, S. Tajik, Voltammetric determination of Bisphenol A in water and juice using a lanthanum (III)-doped cobalt (II, III) nanocube modified carbon screen-printed electrode. *Anal. Lett.* **52**, 1432–1444 (2019)
 45. H. Zhou, L. Chen, S. Li, S. Huang, Y. Sun, Y. Chen, Z. Wang, W. Liu, X. Li, One-step electroreduction preparation of multilayered reduced graphene oxide/gold-palladium nanohybrid as a proficient electrocatalyst for development of sensitive hydrazine sensor. *J. Colloid Interface Sci.* **566**, 473–484 (2020)
 46. S.Z. Mohammadi, H. Beitollahi, E. BaniAsadi, Electrochemical determination of hydrazine using a ZrO_2 nanoparticles-modified carbon paste electrode. *Environ. Monit. Assess.* **187**, 122 (2015)
 47. Y. Dong, C. Duan, J. Zheng, Controlled synthesis of Material of Institute Lavoisier-53(Fe) for amperometric determination of hydrazine. *J. Electroanal. Chem.* **873**, 114407 (2020)
 48. Y. Ran, Y. Li, X. Cui, T. Lai, L. Yao, R. Zhao, L. Wang, Y. Wang, Sm-doped SnO_2 nanoparticles synthesized via solvothermal method as a high-performance formaldehyde sensing material for gas sensors. *J. Mater. Sci.* **32**, 8249–8264 (2021)
 49. H.-A. Kalaleh, K. Masri, The role of butanol isomers on the performance of ammonia sensors based on polypyrrole prepared by microemulsion polymerization. *J. Mater. Sci.* **32**, 8978–8988 (2021)
 50. C. Wang, D. Ding, X. Jiang, B. Zhou, Electrochemical sensors based on copper-cadmium bimetallic porphyrin coordination polymers with various Cu/Cd ratios. *J. Anal. Chem.* **76**, 772–778 (2021)
 51. L. Zhao, H. Shang, B. Tian, D. Wang, Y. Liu, W. Wang, Manufacturability and reliability optimization for metallization of SiC piezoresistive pressure sensors. *J. Mater. Sci: Mater. Electron.* **32**, 17637–17644 (2021)
 52. D. Guettiche, A. Mekki, B. Lilia, T. Fatma-Zohra, A. Boudjellal, Flexible chemiresistive nitrogen oxide sensors based on a nanocomposite of polypyrrole-reduced graphene oxide-functionalized carboxybenzene diazonium salts. *J. Mater. Sci: Mater. Electron.* **32**, 10662–10677 (2021)
 53. M. Mokni, N. Fourati, C. Zerrouki, A. Othmane, A. Omezine, A. Bouslama, Review on recent advances in urinary biomarkers based electrochemical sensors for prostate cancer detection, in *Advanced Sensors for Biomedical Applications Smart Sensors, Measurement and Instrumentation*, vol. 38, ed. by O. Kanoun, N. Derbel (Springer, Cham, 2021)
 54. A.A. Abdul-Hamead, F.M. Othman, M.A. Fakhri, Preparation of MgO-MnO_2 nanocomposite particles for cholesterol sensors. *J. Mater. Sci: Mater. Electron.* **32**, 15523–15532 (2021)
 55. C.T. Thanh, N.H. Binh, P.N. Duc Duoc, V.T. Thu, P.V. Trinh, N.N. Anh, N.V. Tu, N.V. Tuyen, N.V. Quynh, V.C. Tu, B.T. Phuong Thao, P.D. Thang, H. Abe, N.V. Chuc, Electrochemical sensor based on reduced graphene oxide/double-walled carbon nanotubes/octahedral Fe_3O_4 /chitosan composite for glyphosate detection. *Bull Environ. Contam. Toxicol.* **106**, 1017–1023 (2021)
 56. Y.-W. Bai, G. Shi, J. Gao, F.-N. Shi, MOF decomposed for the preparation of $\text{Co}_3\text{O}_4/\text{N}$ -doped carbon with excellent microwave absorption. *J. Solid State Chem.* **288**, 121401 (2020)
 57. P.Y. Chu, C. Tian, Q. Yao, Effects of Co element on the structure, magnetic, and microwave absorption properties of La-Fe-B alloys. *J. Supercond. Nov. Magn.* **33**, 1125–1128 (2020)
 58. S.Z. Mohammadi, H. Beitollahi, H. Allahabadi, T. Rohani, Disposable electrochemical sensor based on modified screen-printed electrode for sensitive cabergoline quantification. *J. Electroanal. Chem.* **847**, 113223 (2019)
 59. Y. Xu, Y. Peng, X. Zheng, K.D. Dearn, H. Xu, X. Hu, Synthesis and tribological studies of nanoparticle additives for pyrolysis bio-oil formulated as a diesel fuel. *Energy* **83**, 80–88 (2015)
 60. F.L.S. Carvalho, Y.J.O. Asencios, A.M.B. Rego, E.M. Assaf, Hydrogen production by steam reforming of ethanol over $\text{Co}_3\text{O}_4/\text{La}_2\text{O}_3/\text{CeO}_2$ catalysts synthesized by one-step polymerization method. *Appl. Catal. A* **483**, 52–62 (2014)
 61. A.J. Bard, L.R. Faulkner, *Electrochemical Methods: Fundamentals and Applications*, 2nd edn. (Wiley, New York, 2001), pp. 100–137
 62. S. Liang, T. Zhou, Y. Gao, Q. Wang, Facile synthesis of $\text{Co}_3\text{O}_4/\text{N}$ -doped carbon nanocomposites as efficient electrode

- material for sensitive determination of hydrazine. *J. Alloys Compd.* **816**, 152574 (2020)
63. J. Li, H. Xie, L. Chen, A sensitive hydrazine electrochemical sensor based on electrodeposition of gold nanoparticles on choline film modified glassy carbon electrode. *Sens. Actuator B* **153**, 239–245 (2011)
64. L. Wang, T. Meng, H. Jia, Y. Feng, T. Gong, H. Wang, Y. Zhang, Electrochemical study of hydrazine oxidation by leaf-shaped copper oxide loaded on highly ordered mesoporous carbon composite. *J. Colloid Interf. Sci.* **549**, 98–104 (2019)
65. T. Hosseinzadeh Sanatkar, A. Khorshidi, E. Sohoul, J. Janczak, Synthesis, crystal structure, and characterization of two Cu(II) and Ni(II) complexes of a tetradentate N_2O_2 Schiff base ligand and their application in fabrication of a hydrazine electrochemical sensor. *Inorg. Chim. Acta* **506**, 119537 (2020)
66. F. Asadi, S.N. Azizi, S. Ghasemi, Preparation of Ag nanoparticles on nano cobalt-based metal organic framework (ZIF-67) as catalyst support for electrochemical determination of hydrazine. *J. Mater. Sci.* **30**, 5410–5420 (2019)
67. Z. Meng, M. Li, X. Liu, Z. Lei, Sensitive electrochemical sensor for hydrazine based on in situ synthesis of $Cu_3(BTC)_2/GO$ nanocomposite. *J. Mater. Sci.* **30**, 18617–18625 (2019)
68. M. Gharani, A. Bahari, S. Ghasemi, Preparation of MoS_2 -reduced graphene oxide/Au nanohybrid for electrochemical sensing of hydrazine. *J. Mater. Sci.* **32**, 7765–7777 (2021)

Publisher's Note Springer Nature remains neutral with regard to jurisdictional claims in published maps and institutional affiliations.